Economic Geology

BULLETIN OF THE SOCIETY OF ECONOMIC GEOLOGISTS

SOCIETY OF ECONOMIC GEOLOGISTS FOUNDED 1920

www.segweb.org

MAY 2008 VOLUME 103 / NUMBER 3

NEOPROTEROZOIC LUFILIAN FORELAND, DEMOCRATIC REPUBLIC OF CONGO

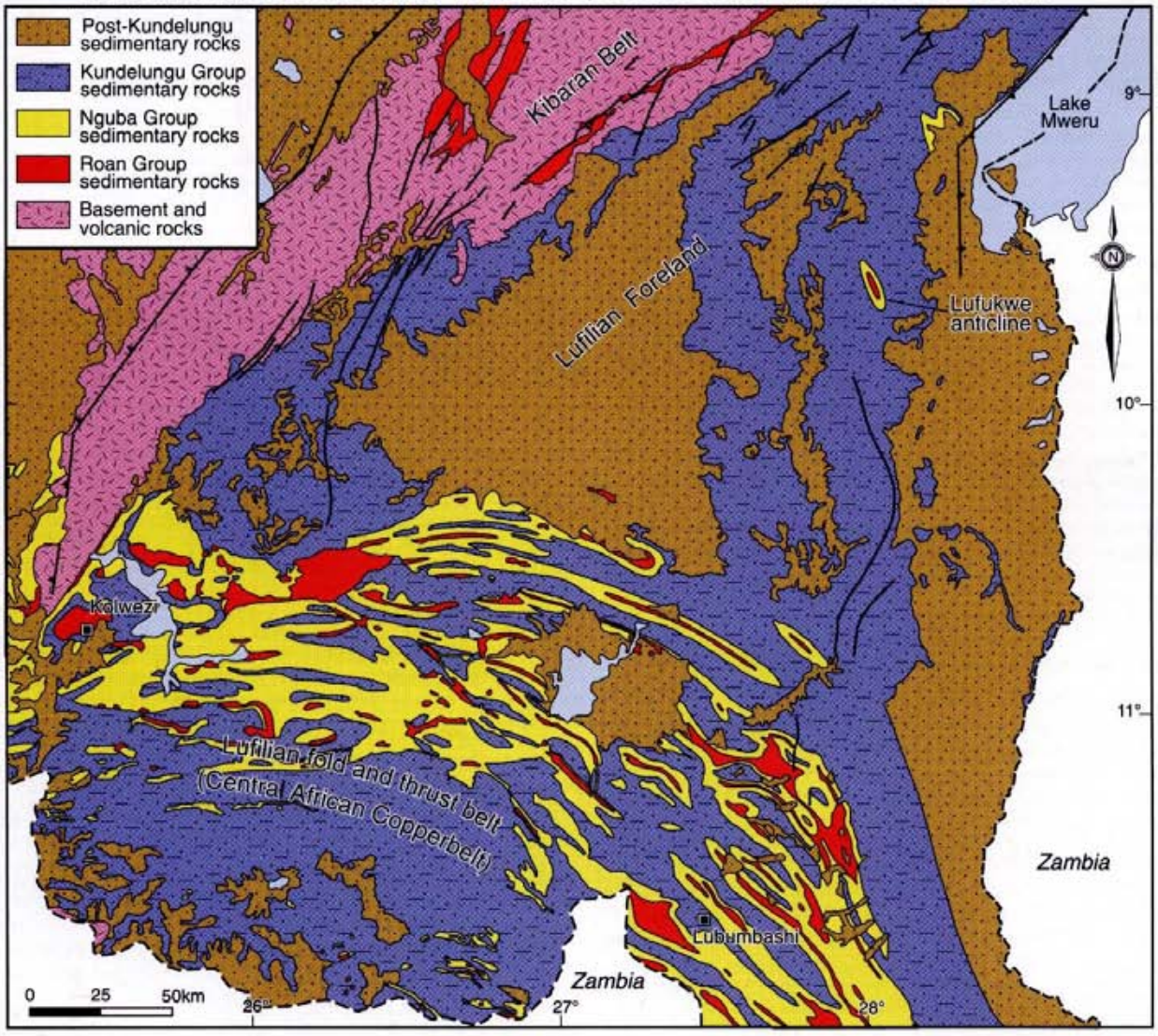

IN THIS ISSUE

CONTENTS

ECGLAL 103(3) 465–660 ISSN 0361-0128

Economic Geology

BULLETIN OF THE SOCIETY OF ECONOMIC GEOLOGISTS

VOL. 103 May 2008 No. 3

EXPRESS LETTER

PRECISE AGE OF THE PLATINIFEROUS MERENSKY REEF, BUSHVELD COMPLEX, SOUTH AFRICA, BY THE U-Pb ZIRCON CHEMICAL ABRASION ID-TIMS TECHNIQUE°

JAMES S. SCOATES† AND RICHARD M. FRIEDMAN

Pacific Centre for Isotopic and Geochemical Research, Department of Earth and Ocean Sciences, University of British Columbia, 6339 Stores Road, Vancouver, British Columbia V6T-1Z4, Canada

Abstract

The Bushveld Complex, South Africa, is the world's largest layered intrusion and host to the majority of the known resources of platinum group elements, chromium, and vanadium. Despite intensive study, determining the precise crystallization age of the Bushveld Complex has proven to be difficult. In this study, zircon and rutile were identified in thin section and separated from a sample of pegmatitic feldspathic orthopyroxenite from the PGE-rich Merensky reef, West mine (Townlands shaft), Rustenburg section. Low U (21–105 ppm) zircon occurs with interstitial biotite and is locally in direct contact with sulfide. Rutile occurs mainly as inclusions within or overgrowths on chromite, especially in the chromitite stringers that bound the reef, and also as acicular grains with biotite. A U-Pb crystallization age of 2054.4 ± 1.3 Ma was determined from single-crystal chemical abrasion ID-TIMS U-Pb dating of zircon, and multigrain fractions of rutile yielded a U-Pb cooling age of 2055.0 ± 3.9 Ma. Integration of the Merensky reef crystallization age with existing U-Pb age determinations for intrusions that pre- and postdate emplacement and crystallization of the layered rocks of the Bushveld Complex indicate that magmatism occurred at ca. 2054 Ma and is contemporaneous with related magmatic activity across the northern Kaapvaal craton of South Africa and Botswana.

Economic Geology, v. 103, pp. 473–491

Hydrothermal Evolution of the Porphyry Copper Deposit at La Caridad, Sonora, Mexico, and the Relationship with a Neighboring High-Sulfidation Epithermal Deposit

VICTOR A. VALENCIA,† CHRISTOPHER EASTOE, JOAQUÍN RUIZ,

Department of Geosciences, University of Arizona, Tucson, Arizona 85721

LUCAS OCHOA-LANDIN,

Departamento de Geología, Universidad de Sonora, Rosales y Transversal, Hermosillo, México

GEORGE GEHRELS,

Department of Geosciences, University of Arizona, Tucson, Arizona 85721

CARLOS GONZÁLEZ-LEON,

Estación Regional del Noroeste, Universidad Nacional Autónoma de México (UNAM), Hermosillo Sonora, México

FERNANDO BARRA,

Department of Geosciences, University of Arizona, Tucson, Arizona 85721, and Instituto de Geologia Economica Aplicada, Universidad de Concepción, Chile

AND ENRIQUE ESPINOZA

Grupo Mexico, Unidad La Caridad, Sonora, Mexico

Abstract

Four main stages of alteration and mineralization are present at La Caridad, Sonora, Mexico. In stage I, quartz veins are associated with orthoclase-anhydrite-biotite hydrothermal alteration within the La Caridad intrusive complex and with pervasive biotitization in andesites and diorites. A zone of propylitic alteration surrounds this biotitic zone. Weak molybdenite ± chalcopyrite ± magnetite ± pyrite ± sphalerite mineralization formed in stage I. stage II, the main hydrothermal mineralization event, is represented by quartz veins with pyrite-sericite + chlorite and is associated with chalcopyrite + pyrite ± molybdenite. In stage III, lead-zinc-silver mineralization formed in veins that were emplaced peripherally to the main system, locally overprinting the earlier events. In stage IV, intermediate-sulfidation mineralization, represented by quartz-tennantite-chalcopyrite-pyrite-sericite veinlets, formed in the core of the porphyry deposit system. The La Caridad Antigua mine, located ~3 km east of the La Caridad orebody, has a high-sulfidation epithermal assemblage that includes pyrophillite, kaolinite, alunite, quartz, and barite as gangue, and a variety of sulfides including, chalcopyrite, pyrite, enargite, tetrahedrite-tennantite, and chalcocite. A new $^{206}Pb/^{238}U$ age of zircons from an associated porphyry stock at La Caridad Antigua is 55.0 ± 1.7 Ma, identical to previous U/Pb ages determined in the porphyry Cu deposit and consistent with a spatial and temporal link between La Caridad and La Caridad Antigua deposits. Fluid inclusion data indicate that stages I and II at La Caridad were deposited by saline hydrothermal fluid at 360° to 460° and 330° to 410°C, respectively. stages III and IV were deposited by low-salinity hydrothermal fluid at 330° to 370° and 260° to 320°C, respectively. Oxygen and hydrogen isotopes indicate deposition of stages I, II, and IV either from magmatic vapor or from mixtures of magmatic and highly evaporated (lacustrine?) formation water and mixing with meteoric water in stages II and III. Sulfur and oxygen isotopes in stage 1 anhydrite indicate external derivation of sulfate and mixing of igneous and external water sources.

Economic Geology, v. 103, pp. 493–537

Mineral Zoning and Geochemistry of Epithermal Polymetallic Zn-Pb-Ag-Cu-Bi Mineralization at Cerro de Pasco, Peru*

REGINA BAUMGARTNER[†,**] LLUÍS FONTBOTÉ,

Department of Mineralogy, University of Geneva, 13 Rue des Maraichers, 1205 Genève, Switzerland

AND TORSTEN VENNEMANN

Institute of Mineralogy and Geochemistry, University of Lausanne Anthropole, 1015 Lausanne, Switzerland

Abstract

The large Cerro de Pasco Cordilleran base metal deposit in central Peru is located on the eastern margin of a middle Miocene diatreme-dome complex and comprises two mineralization stages. The first stage consists of a large pyrite-quartz body replacing Lower Mesozoic Pucará carbonate rocks and, to a lesser extent, diatreme breccia. This body is composed of pyrite with pyrrhotite inclusions, quartz, and black and red chalcedony (containing hypogene hematite). At the contact with the pyrite-quartz body, the diatreme breccia is altered to pyrite-quartz-sericite-pyrite. This body was, in part, replaced by pipelike pyrrhotite bodies zoned outward to carbonate-replacement Zn-Pb ores bearing Fe-rich sphalerite (up to 24 mol % FeS).

The second mineralization stage is partly superimposed on the first and consists of zoned east-west–trending Cu-Ag-(Au-Zn-Pb) enargite-pyrite veins hosted in the diatreme breccia in the western part of the deposit and well-zoned Zn-Pb-(Bi-Ag-Cu) carbonate-replacement orebodies; in both cases, sphalerite is Fe poor and the inner parts of the orebodies show typically advanced argillic alteration assemblages, including aluminum phosphate sulfate (APS) minerals. The zoned enargite-pyrite veins display mineral zoning, from a core of enargite-pyrite ± alunite with traces of Au, through an intermediate zone of tennantite, chalcopyrite, and Bi minerals to a poorly developed outer zone bearing sphalerite-galena ± kaolinite. The carbonate-hosted replacement ores are controlled along N35°E, N 90° E, N 120° E, and N 170° E faults. They form well-zoned upward-flaring pipelike orebodies with a core of famatinite-pyrite and alunite, an intermediate zone with tetrahedrite-pyrite, chalcopyrite, matildite, cuprobismutite, emplectite, and other Bi minerals accompanied by APS minerals, kaolinite, and dickite, and an outer zone composed of Fe-poor sphalerite (in the range of 0.05–3.5 mol % FeS) and galena. The outermost zone consists of hematite, magnetite, and Fe-Mn-Zn-Ca-Mg carbonates. Most of the second-stage carbonate-replacement orebodies plunge between 25° and 60° to the west, suggesting that the hydrothermal fluids ascended from deeper levels and that no lateral feeding from the veins to the carbonate-replacement orebodies took place.

In the Venencocha and Santa Rosa areas, located 2.5 km northwest of the Cerro de Pasco open pit and in the southern part of the deposit, respectively, advanced argillic altered dacitic domes and oxidized veins with advanced argillic alteration halos occur. The latter veins are possibly the oxidized equivalent of the second-stage enargite-pyrite veins located in the western part of the deposit.

The alteration assemblage quartz-muscovite-pyrite associated with the pyrite-quartz body suggests that the first stage precipitated at slightly acidic pH. The sulfide mineral assemblages define an evolutionary path close to the pyrite-pyrrhotite boundary and are characteristic of low-sulfidation states; they suggest that the oxidizing, slightly acidic hydrothermal fluid was buffered by phyllite, shale, and carbonate host rock. However, the presence in the pyrite-quartz body of hematite within quartz suggests that, locally, the fluids were less buffered by the host rock. The mineral assemblages of the second mineralization stage are characteristic of high- to intermediate-sulfidation states. High-sulfidation states and oxidizing conditions were achieved and maintained in the cores of the second-stage orebodies, even in those replacing carbonate rocks. The observation that, in places, second-stage mineral assemblages are found in the inner and outer zones is explained in terms of the hydrothermal fluid advancing and waning.

Microthermometric data from fluid inclusions in quartz indicate that the different ores of the first mineralization stage formed at similar temperatures and moderate salinities (200°–275°C and 0.2–6.8 wt % NaCl equiv in the pyrite-quartz body; 192°–250°C and 1.1–4.3 wt % NaCl equiv in the pyrrhotite bodies; and 183°–212°C and 3.2–4.0 wt % NaCl equiv in the Zn-Pb ores). These values are similar to those obtained for fluid inclusions in quartz and sphalerite from the second-stage ores (187°–293°C and 0.2–5.2 wt % NaCl equiv in the enargite-pyrite veins; 178°–265°C and 0.2–7.5 wt % NaCl equiv in quartz of carbonate-replacement orebodies; 168°–222°C and 3–11.8 wt % NaCl equiv in sphalerite of carbonate-replacement orebodies; and 245°–261°C and 3.2–7.7 wt % NaCl equiv in quartz from Venencocha). Oxygen and hydrogen isotope compositions on kaolinite from carbonate-replacement orebodies ($\delta^{18}O$ = 5.3–11.5‰, δD = –82 to –114‰) and on alunite from the Venencocha and Santa Rosa areas ($\delta^{18}O$ = 1.9–6.9‰, δD = –56 to –73‰). Oxygen isotope compositions of quartz from the first and second stages have $\delta^{18}O$ values from 9.1 to 17.8 per mil. Calculated fluids in equi-

[†] Corresponding author: e-mail, regina.baumgartner@teckcominco.com

*A digital supplement to this paper is available at <http://www.geoscienceworld.org/> or, for members and subscribers, on the SEG website, <http://www.segweb.org>.

**Present address: Teck Cominco Peru, Psje. los Delfines 159, Las Gardenias, Santiago de Surco Lima 33, Peru.

librium with kaolinite have $\delta^{18}O$ values of 2.0 to 8.2 and δD values of –69 to –97 per mil; values in equilibrium with alunite are –1.4 to –6.4 and –62 to –79 per mil. Sulfur isotope compositions of sulfides from both stages have a narrow range of $\delta^{34}S$ values, between –3.7 and +4.2 per mil; values for sulfates from the second stage are between 4.2 and 31.2 per mil. These results define two mixing trends for the ore-forming fluids. The first trend reflects mixing between a moderately saline (~10 wt % NaCl equiv) magmatic end member that had degassed (as indicated by the low δD values) and meteoric water. The second mixing indicates condensation of magmatic vapor with HCl and SO_2 into meteoric water, which formed alunite.

The hydrothermal system at Cerro de Pasco was emplaced at a shallow depth (~500 m) in the epithermal and upper part of a porphyry environment. The similar temperatures and salinities obtained for the first stage and second stages, together with the stable isotope data, indicate that both stages are linked and represent successive stages of epithermal polymetallic mineralization in the upper part of a porphyry system.

Economic Geology, v. 103, pp. 539–554

Synthetic Fluid Inclusions. XVII.[1] PVTX Properties of High Salinity H_2O-NaCl Solutions (>30 wt % NaCl): Application to Fluid Inclusions that Homogenize by Halite Disappearance from Porphyry Copper and Other Hydrothermal Ore Deposits[**]

S. P. Becker,[†*] A. Fall, and R. J. Bodnar

Fluids Research Laboratory, Department of Geosciences, Virginia Polytechnic Institute and State University, Blacksburg, Virginia 24061

Abstract

Fluid inclusions that homogenize by disappearance of the halite crystal after the vapor bubble has disappeared have been reported from a wide range of ore-forming systems. While this inclusion type is most commonly observed in porphyry copper and similar magmatic-hydrothermal ore deposits, they have also been reported from iron oxide copper-gold (IOCG), Mississippi Valley-type, orogenic (lode, greenstone) gold, massive sulfide, unconformity U, and manto-type deposits, as well as from non-ore associated granitoids and oceanic crust. The lack of experimental data to interpret microthermometric data from these inclusions, combined with poor petrographic characterization of inclusion origin, has led to a wide range of inferred PT trapping conditions for the inclusions.

The relationship between liquid-vapor homogenization temperature (Th_{L-V}), halite dissolution temperature (Tm_{halite}) and pressure has been determined using synthetic H_2O-NaCl fluid inclusions that homogenize by halite disappearance. The experimental data cover the range $Th_{L-V} \approx 150°$ to 500°C and $Tm_{halite} \approx 275°$ to 550°C. An empirical equation describing the relationship between pressure, Th_{L-V}, and Tm_{halite} has been developed to estimate formation pressures from microthermometric data and is valid from pressures along the liquid + vapor + halite curve to 300 MPa.

A detailed literature review reveals that the results of this study cannot be applied retroactively to estimate pressures of previously reported inclusions that homogenize by halite dissolution for several reasons. First, most workers have not collected and reported the data in a manner that allows one to determine if the inclusions have trapped a single, homogeneous phase and have not leaked or changed volume following trapping. Thus, it is not possible to determine if the inclusions show consistent microthermometric behavior within a group of coeval inclusions. Additionally, many published studies provide only summaries of results from numerous samples or present the data graphically, precluding application of our results to individual inclusions. However, based on our review, it appears that much of the published data for inclusions that homogenize by halite dissolution represent inclusions that have either trapped a halite crystal along with the liquid or have reequilibrated by necking and/or stretching.

Results from this study have been used to estimate minimum formation pressures for inclusions from the Ditrau Alkaline Massif, Transylvania, Romania, the Musoshi stratiform copper deposit, Zaire, the Bismark skarn deposit, northern Mexico, the Naica chimney-manto deposit, Mexico, the Questa porphyry molybdenum deposit, New Mexico, and the Bingham Canyon porphyry Cu-Mo deposit, Utah. In each case, pressures estimated using results from the present study are in good agreement with previous pressure estimates. However, in some cases estimated pressures (both our estimates as well as those of other authors) appear to be unreasonably high, based on the geologic setting at the time of formation. These results highlight the currently limited understanding concerning pressures (depths) of ore formation.

Economic Geology, v. 103, pp. 555–582

Postorogenic Origin of the Stratiform Cu Mineralization at Lufukwe, Lufilian Foreland, Democratic Republic of Congo

HAMDY A. EL DESOUKY,† PHILIPPE MUCHEZ,

Geodynamics and Geofluids Research Group, K.U. Leuven, Celestijnenlaan 200E, B-3001 Leuven, Belgium

STIJN DEWAELE,

Department of Geology and Mineralogy, Royal Museum of Central Africa (RMCA), Leuvensesteenweg 13, 3080 Tervuren, Belgium

AMANDA BOUTWOOD, AND ROGER TYLER

ANVIL MINING CONGO SARL, 8034 Avenue Nyota, Quartier Golf, Lumbumbashi, Democratic Republic of Congo

Abstract

The Central African Copperbelt, which stretches across the border between Zambia and the Democratic Republic of Congo, is one of the largest sediment-hosted stratiform Cu-Co provinces in the world. The triangular-shaped Lufilian foreland is located to the northeast of the Copperbelt. Recently sediment-hosted stratiform copper occurrences have been explored in the foreland, including the Kinkumbi prospect in the Lufukwe anticline. Although the stratiform copper mineralization in the Copperbelt is mainly concentrated in the Roan Group sedimentary rocks, where it is commonly associated with cobalt, the Lufilian foreland copper mineralization occurs in sedimentary rock units of the Nguba and Kundelungu Groups where it is mainly associated with silver. This paper examines the metallogenesis of the stratiform copper mineralization at Lufukwe.

The Lufukwe anticline is situated in the eastern part of the Lufilian foreland and is composed of Neoproterozoic sedimentary rocks belonging to the Katanga Supergroup. The Kinkumbi prospect, a sediment-hosted stratiform copper-silver occurrence, is located in the northern part of the western flank of the anticline. This part of the anticline is characterized by disseminated copper-silver mineralization hosted in the lower 10 to 15 m of the Monwezi Sandstone (Nguba Group). A comparison between the location of high copper grades in surface samples and boreholes and the location of structural lineaments visible on ASTER images indicates that the mineralization is spatially related to northeast-southwest to east-northeast–west-southwest strike-slip faults. These faults are nearly perpendicular to the strike of the host rock and postdate both the Lufilian folding and deposition of the entire Katanga Supergroup.

The Monwezi Sandstone was subjected to strong compaction and silica cementation (authigenic quartz overgrowths), followed by intense feldspar dissolution, which resulted in a well-developed secondary porosity represented by dissolution cavities. Copper sulfides are mainly concentrated in these cavities and partially replace the detrital grains. The copper mineralization is both hypogene (chalcopyrite, bornite, and chalcocite) and supergene (digenite, covellite, and minor native copper), with malachite and chrysocolla as the main oxidation products. Point counting and grain size measurements demonstrate that the sandstone horizons with high copper content (>1.25% Cu) are those with a detrital grain size larger than 175 μm, more than 35 percent altered feldspars and little or no fine-grained matrix. Microthermometry of fluid inclusions indicates that the authigenic quartz overgrowths precipitated from a moderate-temperature (80°–130°C), high-salinity (18.8–23.4 wt % $CaCl_2$ equiv) H_2O-NaCl-$CaCl_2$ fluid. The hypogene copper-silver mineralization was deposited from a hot (120°–180°C) and low- to moderate-salinity (1.9–7.7 wt % NaCl equiv) H_2O-NaCl fluid with a general trend of increasing homogenization temperatures with increasing salinities. The interpretation of the available structural, stratigraphic, petrographic, and fluid inclusion microthermometric data constrain the timing of the mineralization to a time after the Lufilian folding and deposition of the entire Katanga Supergroup.

The data presented support a postorogenic fluid-mixing model in which the mineralization is related to the mixing of a copper-rich mineralizing fluid with a temperature ≥180°C and salinity ≥7.7 wt percent NaCl equiv, likely migrating upward along northeast-southwest– to east-northeast–west-southwest–oriented strike-slip faults, with a colder, low-salinity, reducing fluid in the Monwezi Sandstone. The location and distance between the northeast-southwest to east-northeast–west-southwest faults strongly influenced the spatial distribution of the copper mineralization in the anticline, and the variability in grain size and composition of the Monwezi Sandstone caused the preferential lateral migration of the mineralizing fluid through the lower 10 to 15 m. Copper precipitation was possibly induced by reduction by preexisting noncopper sulfides (pyrite and arsenopyrite) and hydrocarbons and by the drop in fluid temperature and salinity. Based on this research the areas with dominant northeast-southwest to east-northeast–west-southwest structural lineaments are considered favorable sites for further copper exploration in the Lufilian foreland, especially where these lineaments cut previously deformed Katanga sediments. Coarse-grained sandstones with no fine matrix that underwent intense feldspar dissolution are the most promising host rocks for the late disseminated stratiform copper mineralization in the Lufilian foreland. Airborne gamma-ray spectrometric surveys could be used as a powerful exploration tool for targeting ore-related, K-depleted zones in these sandstones.

† Corresponding author: e-mail, HamdyAhmed.ElDesouky@geo.kuleuven.be

0361-0128/08/3741/555-28

Economic Geology, v. 103, pp. 583–598

Uranium Metallogenesis in South China and Its Relationship to Crustal Extension during the Cretaceous to Tertiary

RUI-ZHONG HU,† XIAN-WU BI,

State Key Laboratory of Ore Deposit Geochemistry, Institute of Geochemistry, Chinese Academy of Sciences, Guiyang 550002, China

MEI-FU ZHOU,

Department of Earth Sciences, University of Hong Kong, Hong Kong, China

JIAN-TANG PENG, WEN-CHAO SU, SHEN LIU, AND HUA-WEN QI

State Key Laboratory of Ore Deposit Geochemistry, Institute of Geochemistry, Chinese Academy of Sciences, Guiyang 550002, China

Abstract

South China is rich in vein-type hydrothermal uranium deposits hosted in granitic, volcanic, and carbonaceous and siliceous pelitic sedimentary rocks. The uranium deposits are spatially associated with extensional structures and/or mantle-derived mafic dikes. Both the uranium deposits and mafic dikes are Cretaceous to Tertiary in age, temporally coincident with the crustal extension. Carbon isotope analyses of calcite deposited in the main-stage mineralization in the veins from 12 representative uranium deposits yield $\delta^{13}C$ values of ore-forming fluids mainly from –4 to –8 per mil, which are permissive of a mantle origin for the CO_2 in the ore-forming fluids. A mantle origin is consistent with the association of the deposits with mafic dikes and the $^3He/^4He$ ratios of ore-forming fluids (e.g., 0.10–2.02 Ra for the volcanic-hosted Xiangshan uranium deposit). Isotopic compositions of H and O demonstrate that water in the ore-forming fluids is predominantly meteoric in origin. Ore-forming temperatures ranged approximately from 150° to 250°C.

Uranium-rich crustal rocks in South China may have been the sources for the uranium. Crustal extension and associated mafic magmatism are considered to have heated the rocks and allowed CO_2 (possibly from mantle sources) to migrate upward and to mix with CO_2-poor meteoric water. The CO_2-rich hydrothermal fluids mobilized uranium from the source rocks and then the uranium was deposited in various host rocks to form the uranium deposits.

Economic Geology, v. 103, pp. 599–614

Bimodal Distribution of Gold in Pyrite and Arsenopyrite: Examples from the Archean Boorara and Bardoc Shear Systems, Yilgarn Craton, Western Australia

ANTHONY A. MOREY,

*predictive mineral discovery*Cooperative Research Centre, School of Geosciences, Monash University, Clayton, Victoria 3800, Australia*

ANDREW G. TOMKINS,†

School of Geosciences, P.O. Box 28E, Monash University, Clayton, Victoria 3800, Australia

FRANK P. BIERLEIN,

Centre for Exploration Targeting and Tectonics Special Research Centre, School of Earth and Geographical Sciences, University of Western Australia, Crawley, Western Australia 6009, Australia

ROBERTO F. WEINBERG,

School of Geosciences, Monash University, Clayton, Victoria 3800, Australia

AND GARRY J. DAVIDSON

ARC Centre of Excellence in Ore Deposits, School of Earth Sciences, University of Tasmania, Hobart, Tasmania 7001, Australia

Abstract

This study investigates the microstructures, geochemistry, and hydrothermal evolution of gold-bearing pyrite and arsenopyrite from six orogenic gold deposits in the Archean Eastern Goldfields Province, Western Australia. Scanning electron microscope (SEM), electron microprobe (EMP) and laser ablation-inductively coupled plasma-mass spectroscopy (LA-ICP-MS) analyses show that the gold-bearing minerals possess a number of similar textural features, including the occurrence of invisible gold within initial phases of growth, and later-stage visible gold associated with alteration rims. The alteration rims are characterized by a higher-than-average atomic mass (mainly owing to arsenic enrichment) and are preferentially located along fractures and grain boundaries in the pyrite and arsenopyrite. These observations suggest that visible gold formation is associated with hydrothermal alteration of preexisting pyrite and arsenopyrite. Textural observations and LA-ICP-MS data suggest that some invisible gold was remobilized from early-formed pyrite and arsenopyrite to form visible gold during development of these alteration rims. Gold may also have been added by hydrothermal fluids during a later stage of mineralization. In situ geochemistry and phase relationships of alteration rims are used to further constrain the hydrothermal process responsible for formation of alteration rims and visible gold in fractures. Based on sulfide stability relations, our data indicate that development of arsenopyrite alteration rims associated with late-stage visible gold formation was related to an increase in temperature (maximum increase from 310° to 415°C) and up to of sic orders of magnitude increase in sulfur fugacity, whereas changes in oxygen fugacity were less important. LA-ICP-MS analyses show that the relative and absolute variations in selected trace element (Au, Ag, Sb, Bi, Ba, Te, Pb, Co, and Mo) concentrations can also be used to distinguish between unaltered and altered pyrite and arsenopyrite. In general, trace elements within pyrite and arsenopyrite have a relatively uniform distribution, whereas later-stage alteration rims have more variable trace element distributions. Although the observed textures are typical of prograde metamorphic coronae, we suggest that they are the consequence of variations in fluid conditions and chemistry, and that mineralization occurred in response to syn- and/or postpeak metamorphic fluid infiltration.

Economic Geology, v. 103, pp. 615–628

Revisiting the Cumulative Grade-Tonnage Relationship for Major Copper Ore Types

M. D. GERST†

Yale University, Center for Industrial Ecology, 205 Prospect Street, New Haven, Connecticut 06511

Abstract

In order to develop long-term scenarios of copper supply and demand, a grade-tonnage density function model was developed for four major copper ore types. The model was used to create cumulative grade-tonnage curves, representing 1,778 million metric tons (Mt) of mineable copper. These cumulative curves were then validated against 70 years of historical world average ore grade using production input by ore type from 1800 to 2000. Additionally, the curves were used in conjunction with estimates of the ultimate porphyry resource and copper concentration in common rocks to conduct a rough analysis of the validity of the bimodal log-Gaussian distribution hypothesis for the global copper resource base. The resulting analysis did not confirm or refute the hypothesis but did provide guidance as to the way in which data from new resource exploration can be used to address the issue of the ultimate mineable copper resource. As ore deposit grade-tonnage data for other geochemically scarce metals becomes available, the methods described in this paper can serve as a template for further investigations of resource quality.

Economic Geology, v. 103, pp. 629–636

SCIENTIFIC COMMUNICATIONS

TERTIARY TILTING AND DISMEMBERMENT OF THE LARAMIDE ARC AND RELATED HYDROTHERMAL SYSTEMS, SIERRITA MOUNTAINS, ARIZONA

WILLIAM J. A. STAVAST,[†,*]

Center for Mineral Resources, Department of Geosciences, University of Arizona, Tucson, Arizona 85721-0077

ROBERT F. BUTLER,[**]

Department of Geosciences, University of Arizona, Tucson, Arizona 85721-0077

ERIC SEEDORFF, MARK D. BARTON,

Center for Mineral Resources, Department of Geosciences, University of Arizona, Tucson, Arizona 85721-0077

AND CHARLES A. FERGUSON

Arizona Geological Survey, 416 West Congress Street, Suite 100, Tucson, Arizona 85701

Abstract

Multiple lines of evidence, including new and published geologic mapping and paleomagnetic and geobarometric determinations, demonstrate that the rocks and large porphyry copper systems of the Sierrita Mountains in southern Arizona were dismembered and tilted 50° to 60° to the south by Tertiary normal faulting. Repetition of geologic features and geobarometry indicate that the area is segmented into at least three major structural blocks, and the present surface corresponds to oblique sections through the Laramide plutonic-hydrothermal complex, ranging in paleodepth from ~1 to ~12 km.

These results add to an evolving view of a north-south extensional domain at high angles to much extension in the southern Basin and Range, contrast with earlier interpretations that the Laramide systems are largely upright and dismembered by thrust faults, highlight the necessity of restoring Tertiary rotations before interpreting Laramide structural and hydrothermal features, and add to the broader understanding of pluton emplacement and evolution of porphyry copper systems.

Economic Geology, v. 103, pp. 637–651

IMAGE ANALYSIS AND COMPOSITION OF PLATINUM-GROUP MINERALS IN THE J-M REEF, STILLWATER COMPLEX

BÉLINDA CODEL,†

Centre for Exploration Targeting, University of Western Australia, Crawley 6009, Australia

AND SARAH-JANE BARNES

Sciences de la Terre, Université du Québec à Chicoutimi, Québec, Canada G7H 2B1

Abstract

Detailed imaging, bulk geochemical analyses, and laser ablation ICP-MS analyses were conducted on mineralized samples from the platinum-group element (PGE)–bearing J-M reef, Stillwater Complex (Montana). The aims of the study were to determine which phases are the main hosts of the PGE, to examine the textural relationships of the PGE-bearing minerals, and the associated base metal sulfides, silicates, and secondary magnetites. The platinum-group minerals (PGM) observed in the studied samples consist of Pd ± Pt sulfides, Pt-Fe alloy (isoferroplatinum), Pd ± Pt tellurides, and Pd-Cu alloy (skaergaardite) with minor native Pd, [Ru(Ir, Os)S_2] (laurite), and Au-Pd-Ag alloy (palladian electrum). These minerals account for all the Pt, half the Pd, Ru, and Ir, and a smaller proportion of the Os in whole rocks (the balance being found in the base metal sulfide). Most of these PGM are closely associated with base metal sulfides, either included in the base metal sulfide or located at the contact between the base metal sulfide and the silicate or oxide minerals. The textures of the PGM within and at the margins of the base metal sulfide suggest that they exsolved from the sulfides. We suggest that the PGE, Ni, Cu, and Te partitioned into a magmatic sulfide liquid that crystallized into base metal sulfide. The Pt-Fe alloys and some of the Pd sulfides exsolved from the base metal sulfide during desulfurization at fairly high temperatures. In contrast, the skaergaardite and some Pd sulfides are found in association with secondary magnetite and probably formed at relatively low temperatures (~250°–465°C) during a second fluid migration event. The Pd/Pt ratio of the reef (~3.3) is higher than most mafic magmas and the Pd/Pt ratio of the footwall is lower (0.3–0.7). It is possible that some of the Pd in the reef was leached from the underlying rocks and deposited in the reef as PGM associated with secondary magnetite.